IDENTIFICATION OF DIAZINON PROTOMERS WITH ION MOBILITY SPECTROMETER

Mohammad Nabi Karimi
Department of physics, Faculty of education, Alberoni University, Afghanistan

Sayed Ali Aqa Sadat
Department of chemistry, Faculty of education, Alberoni University, Afghanistan

ABSTRACT

Background: Diazinon pesticide is a chemical compound used in agriculture and horticulture and it has been identified and measured by various methods such as mass spectrometer, magnetic spectrometer, chromatography, IR, etc. Due to the chemical structure of diazinon, it can accept protons from active ions and be charged in multiple areas.

Materials and methods: This research is a laboratory study using an ion mobility spectrometer. The obtained data were analyzed using Sigma Plot and ViIms software.

Findings: This research was conducted to investigate the protonation mechanism of diazinon. Due to its proton scavenging properties, diazinon can be detected and measured using an ion mobility spectrometer in positive polarity mode. In this study, a new approach to distinguish between diazinon protomers by observing intramolecular hydrogen bond formation after protonation was introduced. The effect of hydrogen bond formation on the structural and electronic properties of protomers was investigated using density functional theory (DFT).

Keywords: ion mobility, diazinon, protomer, spectroscopy, pesticides.

INTRODUCTION

Diazinon is one of the pesticides used in agriculture and horticulture [1-4]. This chemical compound is an oily and colorless liquid and is one of the organophosphorus pesticides[5, 6]The solubility of diazinon in water at 20°C is 60 mg/liter[3, 7]. This pesticide is sensitive to oxidation conditions and its decomposition is possible at temperatures above 20°C in acidic and alkaline environments[6, 8-10] Many organic molecules have multiple proton binding sites[3, 11] Protonation of a molecule with several sites may lead to the formation of protonic isomers (protomers)[6, 11, 12] Protomers can be identified and studied using different techniques, such as ion mobility spectroscopy, photochemical, and infrared techniques[11, 13] Protomers can be detected and separated by an ion mobility spectrometer, which has two criteria. Comparable relative abundance and different ionic mobility[12, 14] According

to the Boltzmann equation, the relative abundance of two protomers is an exponential function of the difference in protonation of the corresponding proton acceptor centers[15, 16]. Hence, [6]for a molecule with multiple steric centers, only one protomer corresponding to the steric center may be produced. However, some strategies have been proposed that lead to changes in the relative abundance of protomers and the formation of unstable protomers. In an electrospray ionization (ESI) source, by changing the solvent composition, the less basic center may become protonated. Protomers must have different mobilities (K) or collision cross sections (CCS) to be separated by IMS Mobility and CCS depend on the structure of the protomer and its interaction with the drift gas flowing in the drift region of the IMS. Therefore, some parameters, such as dipole moment (μD) and polarizability (α), are determining factors affecting the detection of protomers in IMS [13, 17]. Because in these compounds, protonation from the N site leads to the concentration of charge on the NH3 group and, as a result, the increase of μD, while the protonation of the oxygen atom of the C=O group causes the charge to spread both on C=O and in the benzene ring, which decreases μD. Therefore, the N protomer with a larger μD experiences more interaction with the drift gas molecules, and its IMS peak appears at a higher drift time [12, 16].

1: Experimental part

1-1. Optimum conditions of the IMS device for diazinon identification

To identify diazinon with the ion mobility spectrometer, compressed air was used as the input gas for the device and the corona ionization source in positive polarity. Reactive ions, which include H_3O^+, NH_4^+, and NO^+, as seen in figure (2), the spectra of reactive ions in positive polarity and diazinon appear as two peaks close to each other at 10.57 and 10.37 milliseconds. These two peaks have been used as indicator peaks to identify and measure diazinon with an ion mobility spectrometer.

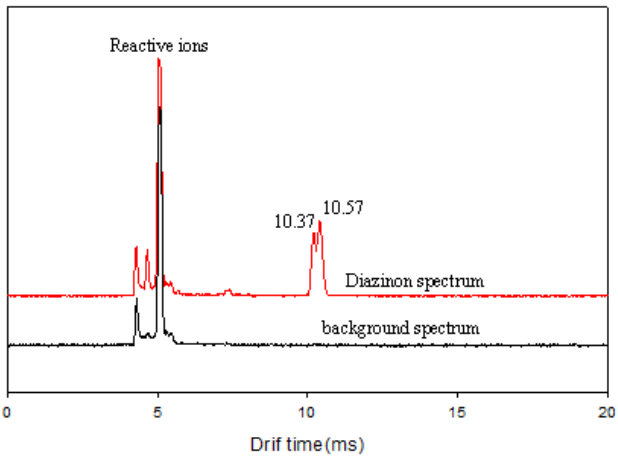

Figure 2: Ion mobility spectrum of diazinon and background spectrum in positive polarity at 200°C and in the presence of air drift gas

1-1. checking the temperature of the injection chamber and thrust tube

Two microliters of 100 ppm diazinon solution were injected into the IMS device at different temperatures in the injection zone (120–260 °C), and their spectra were recorded in Figure 3. The temperature of the injection zone above 120 °C can be used to measure diazinon with the IMS device. The temperature of 260 °C was used as the optimal temperature for diazinon measurement. The temperature of TB was investigated from 30°C to 200°C (Figure 4). An increase in temperature causes an increase in the intensity of the diazinon signal. Therefore, the temperature of 200 °C was chosen as the optimal temperature for measuring diazinon. The increase in ion mobility makes the ions reach the detector earlier, and the peaks appear in a shorter drift time.

Therefore, with the shortening of the time for the ions to reach the detector, the amount of their losses due to hitting each other or the wall is reduced, ultimately leading to an increase in the percentage of ions passing and an increase in the signal.

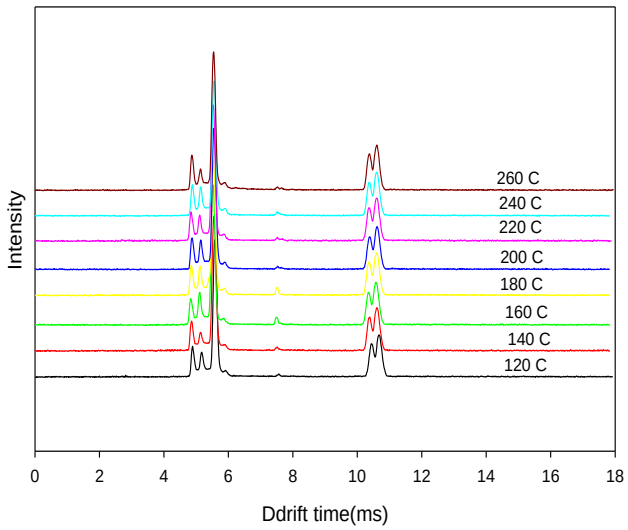

Figure 3: Ion mobility spectrum of diazinon at different temperatures in the injection area

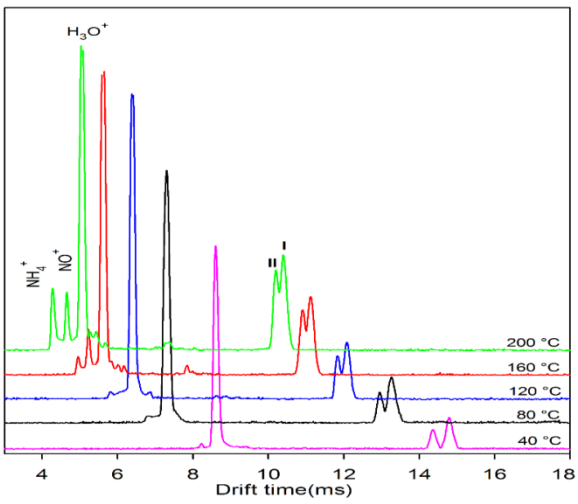

Figure 4: Ion mobility spectrometer of diazinon at different temperatures

Table 1 shows the optimal conditions of the device for identifying and measuring diazinon.

Table 1: optimal parameters of the ion mobility spectrometer device to measure diazinon

IMS device parameters	optimal value
Corona voltage(V)	2300
Thrust area voltage(V)	8000
Thrust tube field(V/cm)	600
Flow rate of thrust area (ml/min)	600
Carrier gas speed (ml/min)	300
Injection chamber temperature (°C)	260
Thrust tube temperature (°C)	200
Pulse width (µs)	50
device polarity	+

1-2. Calibration chart for diazinon measurement

In the spectra recorded with the ion mobility spectrometer in optimal conditions, the area under the diazinon peak at each concentration was calculated using Vis IMS software.

The linear range of the calibration curve for diazinon measurement is 0.1–8 ppm. The linear equation (y=0.0492x+0.0175) was recorded as shown in figure 5.

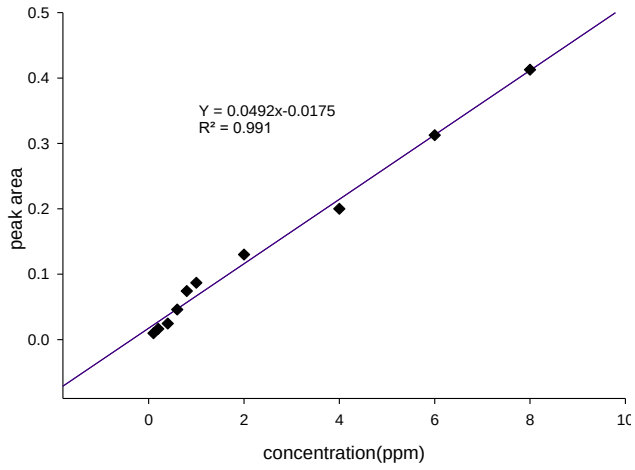

Figure 5: Linear range of the diazinon calibration curve

2: Discussion and results

2-1. Computational details

Optimization of isomers of the diazinon molecule in the gas phase was done using B3LYP and density functional theory (DFT)[18, 19]. Frequency calculations were performed at the same level of theory to obtain thermodynamic functions at 298K[20].

2-2. Investigation of diazinon protomers

At 40°C, two peaks I and II were observed for diazinon at drift times (td) of 14.58 and 14.80 ms. As the temperature increases, the peaks shift to lower drift times. Also, with increasing temperatures, the peak-to-peak distance decreases. Same as Figure 4. Mobility (K) and consequently td depend on temperature according to the Mason-Champ equation in the form of equation (1) .

$$\frac{1}{t_d} = \frac{3}{16}\frac{EqT}{l_d P}\left(\frac{2\pi k}{\mu}\right)^{1/2}\frac{1+\alpha}{\Omega T^{1/2}} \text{.....(1)}$$

q is the baryon, P is the thrust gas pressure, ld and E are the length and electric field of the thrust tube, μ and Ω are the reduced mass of the cross section of the ion/propellant gas collision, k is Boltzmann's constant, and α is a parameter smaller than 0.02. The ion/molecule cross section, Ω, shows a T-1/2 dependence for most systems [11, 10]. Therefore, ΩT1/2 is a parameter independent of temperature. Therefore, td/1 must be a linear function of T. It shows the graphs of td vs. T for peaks I and II of diazinon in Figure 6. 1/td-T plots are two curves with almost the same slope for peaks I and II.

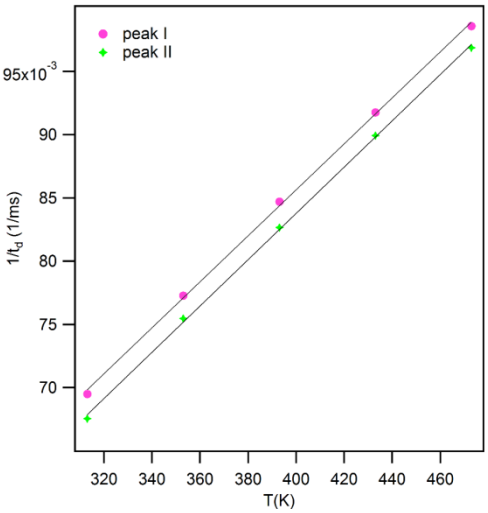

Figure 6: graph of 1/td versus T for peaks I and II of diazinon

The linearity and the same slope of these two curves indicate that these two protomers do not undergo breakage or waterproofing at the studied temperatures. As the temperature increases, peaks I and II may overlap to some extent, which could be due to the structural features described in the following sections.

The optimized structure of four isomers of diazinon (D) is shown in Figure 7. These structures are rotational isomers due to the rotation of the CH (CH3)2 and P

(OC2H5)2 groups. Although the D-b structure is the most stable isomer, due to the small difference in their relative energies, all four structures have considerable abundance.

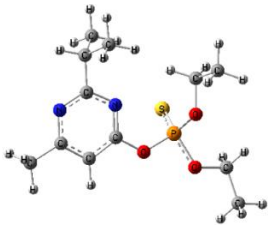

D-a
1.8
27.5%

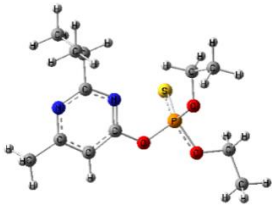

D-b
0.0
57.5%

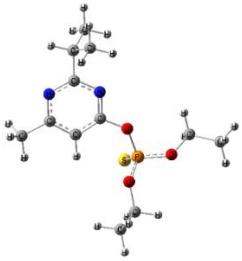

D-c
4.7
8.6%

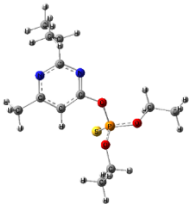

D-d
5.4
6.4%

Figure 7: Optimized structures for different diazinon isomers in the gas phase Relative energy is in kJ/mol.

Diazinon has several centers for proton capture, including the ring N atom, a P=S sulfur atom, and three oxygen atoms attached to the P atom. Protonation of nitrogen atoms leads to the formation of protomers I and II.

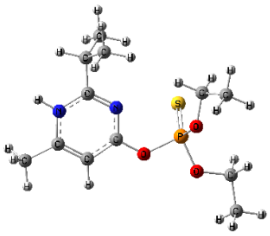

Protomer-Ia
5.5

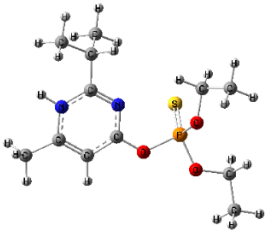

Protomer-Ib
3.9

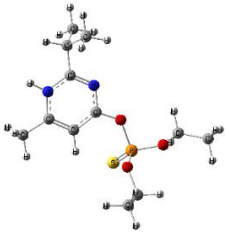

Protomer-Ic
0.0

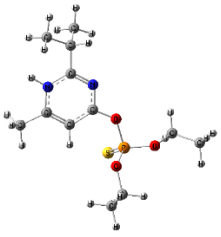

Protomer-Id
1.0

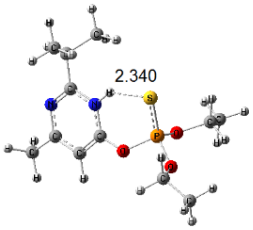

Protomer-IIa
2.6

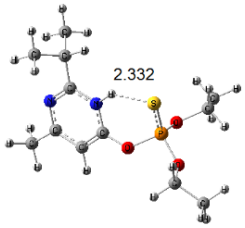

Protomer-IIb
0.9

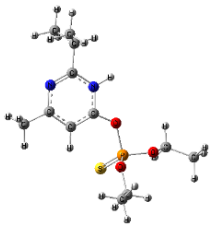

Protomer-IIc
7.3

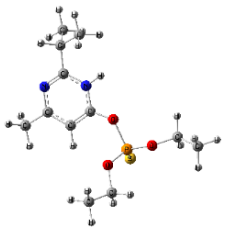

Protomer-IId
7.9

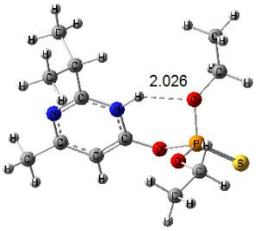

Protomer-IIe
15.0

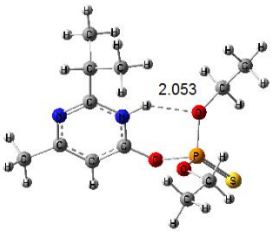

Protomer-IIf
16.8

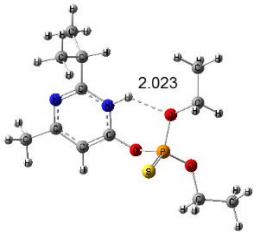

Protomer-IIg
5.5

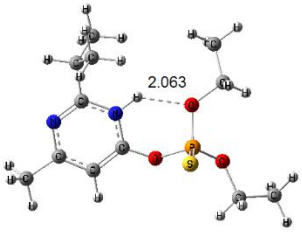

Protomer-IIh
8.2

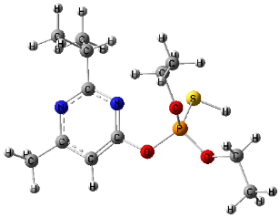

Protomer-IIIa
75.4

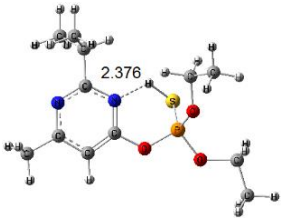

Protomer-IIIb
70.9

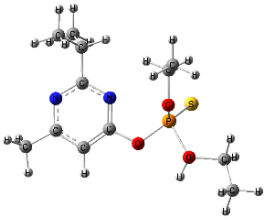

Protomer-IV
150.3

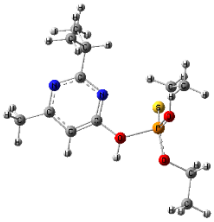

Protomer-V
168.8

Figure 8 shows optimized structures for protonated diazinon isomers in the gas phase. Intramolecular hydrogen bond length and relative energies are in Å and kJ mol-1, respectively.

Protomers III and IV-V are produced from the protonation of S and O centers, respectively. The calculated values of PA and GB for all diazinon centers are summarized in Table 2. The comparison of relative energies shows that the nitrogen atoms inside the ring are the most favorable protonation sites, so that protomers I and II are the most stable protonated structures of diazinon. These protomers are more stable than S-protomers (III) and O-protomers by 75 and 160 kJ bromole, respectively. Therefore, the IMS peak observed in Figure 9 can be attributed to protomers I and II.

Table 2: PA and GB values calculated for all diazinon sites at 298 K in the gas phase

protomer				PA (kJ mol^{-1})	GB (kJ mol^{-1})
D-b Protomer-Ia	+	H^+	→	965/9	936/1
D-b	+	H^+	→	967/5	936/5

Protomer-Ib				
D-b	+	H^+	→	971/4	942/3
Protomer-Ic				
D-b	+	H^+	→	970/4	939/9
Protomer-Id				
D-b	+	H^+	→	968/8	938/9
Protomer-IIa				
D-b	+	H^+	→	970/5	941/9
Protomer-IIb				
D-b	+	H^+	→	964/1	934/6
Protomer-IIc				
D-b	+	H^+	→	963/5	935/0
Protomer-IId				
D-b	+	H^+	→	956/4	930/4
Protomer-IIe				
D-b	+	H^+	→	954/6	923/5
Protomer-IIf				
D-b	+	H^+	→	965/9	937/1
Protomer-IIg				
D-b	+	H^+	→	963/2	933/8
Protomer-IIh				
D-b	+	H^+	→	896/0	869/7
Protomer-IIIa				
D-b	+	H^+	→	900/5	873/9
Protomer-IIIb				
D-b	+	H^+	→	821/1	793/1
Protomer-IV				
D-b	+	H^+	→	802/6	777/7
Protomer-V				

The comparable stability of N-protomers I and II (difference of ~0.9 kJ mol-1) ensures that both protomers are formed with comparable abundance (44:56% at oC200). It should be noted that these N-protomers have different ionic mobility. In protomer II, the incoming proton can form an intramolecular hydrogen bond with adjacent S or O atoms. Figure 1 shows that hydrogen interaction with sulfur atoms (IIa–IIb) is stronger than hydrogen bonding with oxygen atoms (IIe–IIh). The formation of an intramolecular hydrogen bond spreads the positive charge of the incoming proton. Therefore, the

dipole moment is expected to be lower for protomer II than for protomer I. The calculated μD values for diazinon and all its protomers are summarized in Table 3.
Table 3 calculates the values of dipole moment and polarizability for different structures of diazinon and its protomers.

protomer	μ_D (D)	α (Å^3)
D-a	2/216817	214/098667
D-b	2/205559	214/747000
D-c	2/847013	215/208333
D-d	2/772606	215/542000
Protomer-Ia	9/946022	211/082000
Protomer-Ib	9/906875	211/264333
Protomer-Ic	8/357034	212/115000
Protomer-Id	8/410073	212/258000
Protomer-IIa	2/510787	210/191000
Protomer-IIb	2/406036	211/137667
Protomer-IIc	3/560249	211/440333
Protomer-IId	3/923802	210/859667
Protomer-IIe	3/837685	209/904000
Protomer-IIf	4/115805	209/269333
Protomer-IIg	2/654212	211/274000
Protomer-IIh	2/778440	210/29400
Protomer-IIIa	5/624669	207/433667
Protomer-IIIb	4/565308	206/929667
Protomer-IV	8/536008	211/230333
Protomer-V	5/313814	210/953667

For neutral diazinon, μD values are around 2.2–2.8 D, while these values increase significantly for protomer I to D 4.8–9.9. Although II protomers are positively charged, their μD values are comparable to neutral diazinon. It should be noted that apart from forming a hydrogen bond, the location of the proton also affects the value of the dipole moment, as in protomer I, the proton is attached to one side of diazinon, while for protomer II, protonation occurs in the center of the molecule. The dipole moment vectors for the most stable neutral and protonated structures of diazinon are compared in figure 9.

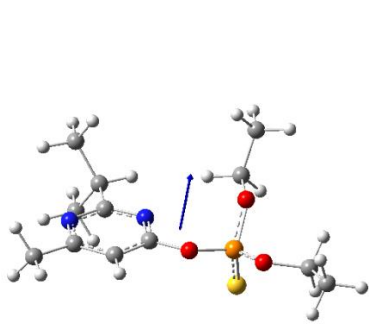

D-b (μ_D = 2.21 D)

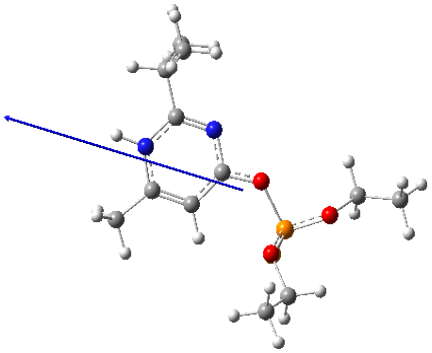

Protomer-Ic (μ_D = 8.36 D)

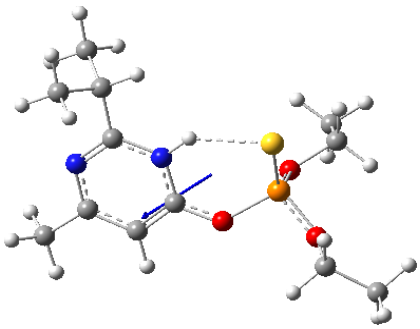

Protomer-IIb (μ_D = 2.41 D)

Figure 9 shows the dipole moment vectors for the most stable structures of protonated and neutral diazinon.

Larger μD values for protomer I lead to a stronger interaction with the drift gas molecules, resulting in the appearance of a peak at higher drift times. In addition, the greater stability of protomers I compared to protomers II makes the intensity of the peak corresponding to protomer I higher than that of protomer II. Peaks I and II in Figure 9 correspond to protomers I and II, respectively. Figure (9) also shows that the relative intensity of peaks I and II changes with temperature. The Boltzmann equation is used to interpret this temperature behavior.

$$\frac{IntensityII}{IntensityI} = \exp(\frac{-\Delta E}{RT}).....(2)$$

According to equation (2), ln (II/I) is a linear function 1/T with a slope of -ΔE/R, where ΔE is the energy difference between protomers I and II and the gas constant R is equal to J mol-1 K-1314. It is 8/ Figure 10 shows the graph of ln (II/I) in terms of 1/T. From the slope of this graph, the energy difference between protomers I and II was equal to 2.6 kJ mol-1, which corresponds to the theoretically calculated value of 0.9 kJ mol-1.

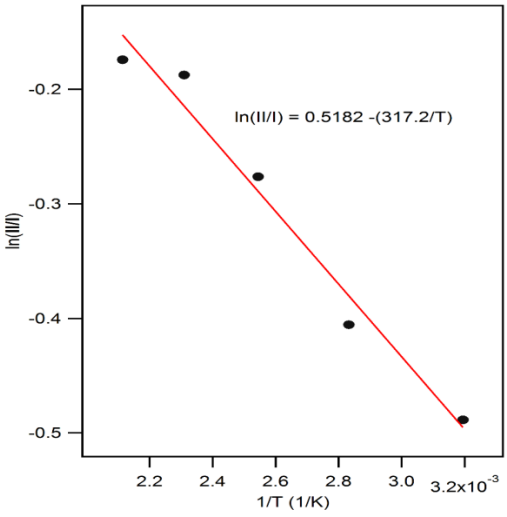

Figure 10 shows the graph of ln(II/I) versus 1/T for the ionic mobility peaks of I and II for diazinon. (II/I) shows the relative intensity of II and I peaks.

Figure (11) shows the potential energy curves for Ic and IIb protomers obtained by scanning the N-C-O-P dihedral angle (group rotation (2P=S (OC2H5)).

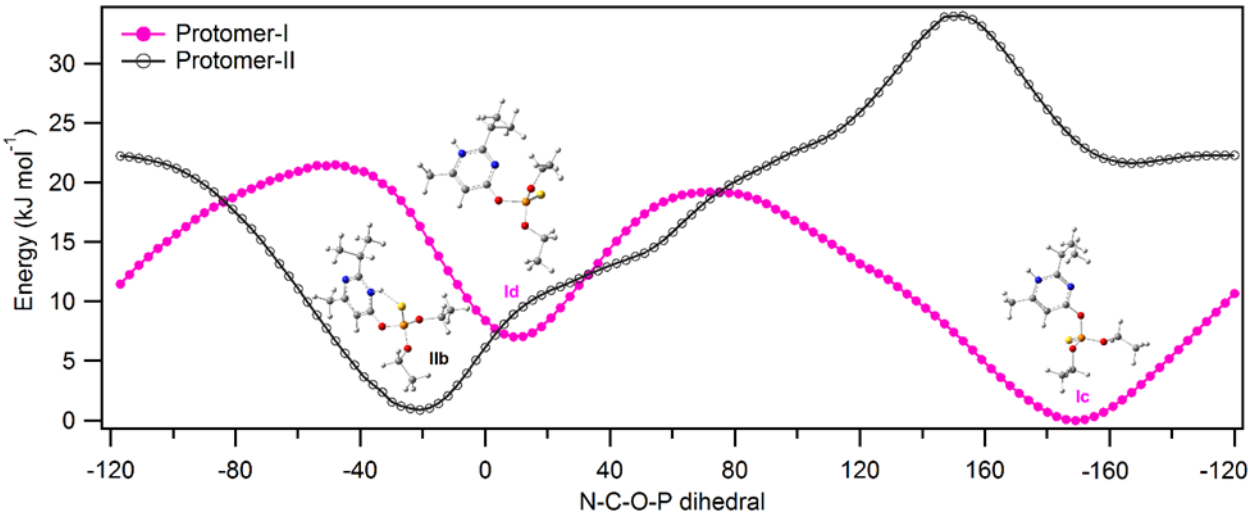

Figure 11: Energy levels obtained for Ic and IIb protomers by N-C-O-P dihedral scan (rotation of the P=S(OC2H5)2 group)

CONCLUSION

As mentioned above, intramolecular hydrogen bond formation in protomer II results in low polarity, less interaction of the ion with the propellant gas, and the appearance of its peak at a lower Td. Intramolecular hydrogen bonding may also affect TD by changing the structure of protomers.

The formation of an intramolecular hydrogen bond in protomer IIb makes the N-C-O-P dihedral angle equal to -20C^{o}[18] In the absence of an intramolecular hydrogen bond (for example, in protomer Ic), the P=S (OC2H5)2 group can rotate to make the N-C-O-P dihedral angle equal to -170o. Intramolecular hydrogen bond formation in isomer IIb produces a rigid structure that cannot easily rotate around the N-C-O-P dihedral, or even if it can overcome the rotational energy and rotate, this rotation does not lead to a stable conformer. Because the potential energy curve does not show any other potential wells for protomer II, But in protomer Ic, because the intramolecular hydrogen bond is not formed, the P=S (OC2H5)2 group can rotate and lead to another stable isomer (Id) with a dihedral angle of N-C-O-P equal to 15°. However, the potential barrier for Ic↔Id conversion is about 19 kJ mol-1, and at high temperatures, the molecule may overcome the energy barrier. In this case, the I peak in the ion mobility spectrum can be related to a mixture of Ic and Id protomers. In short, the formation of a hydrogen bond leads to a change in the structure and polarity of protomer II. The formation

of the NH...S bond in protomer II leads to a stable and strong structure where the P=S(OC2H5)2 group is not able to rotate freely. But in protomer I, without hydrogen bonding, the P=S(OC2H5)2 group can rotate, and interconversion between its two structures is possible. This difference in structure in protomers I and II leads to different ionic mobility and the observation of two separate peaks for two isomers of protonated diazinon.

REFERENCES

1. Solomon, E.I., et al., *Copper active sites in biology.* Chemical reviews, 2014. **114** (7): p. 3659-3853.
2. Ogutcu, A., et al., *The effects of organophosphate insecticide diazinon on malondialdehyde levels and myocardial cells in rat heart tissue and protective role of vitamin E.* Pesticide biochemistry and physiology, 2006. **86**(2): p. 93-98.
3. Sadat, S.A.A., V. Ilbeigi, Y. Valadbeigi, and M. Soleimani, *Determination of pesticides phosalone and diazinon in pistachio using ion mobility spectrometry.* International Journal for Ion Mobility Spectrometry, 2020. **23**: p. 127-131.
4. Pardue, J.R., E.A. Hansen, R.P. Barron, and J.-Y.T. Chen, *Diazinon residues on field-sprayed kale. Hydroxydiazinon---new alteration product of diazinon.* Journal of Agricultural and Food Chemistry, 1970. **18**(3): p. 405-408.
5. Petersson, G.A., et al., *Calibration and comparison of the Gaussian-2, complete basis set, and density functional methods for computational thermochemistry.* The Journal of chemical physics, 1998. **109**(24): p. 10570-10579.
6. Pehkonen, S.O. and Q. Zhang, *The degradation of organophosphorus pesticides in natural waters: a critical review.* Critical reviews in environmental science and technology, 2002. **32**(1): p. 17-72.
7. Marlton, S.J., et al., *Selecting and identifying gas-phase protonation isomers of nicotineH+ using combined laser, ion mobility and mass spectrometry techniques.* Faraday discussions, 2019. **217**: p. 453-475.
8. Lee, S.-R., B.-S. Yoo, and H.-K. Chun, *Bioconcentration of Diazinon and Fenitrothion in Carp (Cyprinus carpio).* Korean Journal of Environmental Agriculture, 1984. **3**(1): p. 30-35.
9. Ahmed, F.E., *Analyses of pesticides and their metabolites in foods and drinks.* TrAC Trends in Analytical Chemistry, 2001. **20**(11): p. 649-661.
10. Ikehata, K. and M. Gamal El-Din, *Aqueous pesticide degradation by ozonation and ozone-based advanced oxidation processes: a review (part II).* Ozone: science & engineering, 2005. **27**(3): p. 173-202.

11. Bisson, M. and A. Hontela, *Cytotoxic and endocrine-disrupting potential of atrazine, diazinon, endosulfan, and mancozeb in adrenocortical steroidogenic cells of rainbow trout exposed in vitro.* Toxicology and Applied Pharmacology, 2002. **180**(2): p. 110-117.
12. Bull, J.N., N.J. Coughlan, and E.J. Bieske, *Protomer-specific photochemistry investigated using ion mobility mass spectrometry.* The Journal of Physical Chemistry A, 2017. **121**(32): p. 6021-6027.
13. Warnke, S., et al., *Protomers of benzocaine: solvent and permittivity dependence.* Journal of the American Chemical Society, 2015. **137**(12): p. 4236-4242.
14. Fu, D., et al., *Understanding of protomers/deprotomers by combining mass spectrometry and computation.* Analytical and Bioanalytical Chemistry, 2023: p. 1-16.
15. Munro, R., *Biosynthetic isotopic labelling strategies for the production of membrane proteins for solid-state Nuclear Magnetic Resonance spectroscopy*. 2021, University of Guelph.
16. McCullagh, M., et al., *Investigations into the performance of travelling wave enabled conventional and cyclic ion mobility systems to characterise protomers of fluoroquinolone antibiotic residues.* Rapid Communications in Mass Spectrometry, 2019. **33**: p. 11-21.
17. Lapthorn, C., et al., *Can ion mobility mass spectrometry and density functional theory help elucidate protonation sites in'small'molecules?* Rapid Communications in Mass Spectrometry, 2013. **27**(21): p. 2399-2410.
18. Valadbeigi, Y., *Effects of intramolecular hydrogen bond and electron delocalization on the basicity of proton sponges and superbases with benzene, pyridine, pyrazine and pyrimidine scaffolds.* Computational and Theoretical Chemistry, 2020. **1188**: p. 112947.
19. Orio, M., D.A. Pantazis, and F. Neese, *Density functional theory.* Photosynthesis research, 2009. **102**: p. 443-453.
20. Paddison, S.J. and E. Tschuikow-Roux, *Structures, vibrational frequencies, thermodynamic properties, and bond dissociation energies of the bromomethanes and bromomethyl radicals: An ab initio study.* The Journal of Physical Chemistry A, 1998. **102**(30): p. 6191-6199.